Low Temperature Physics/Fizika Nizkikh Temperatur, 2019, v. 45, No. 12, pp. 1514–1523

Conductivity of pressed powders of chromium dioxide with spin-dependent electron tunneling: the effect of thickness and composition of dielectric layers

N.V. Dalakova, E.Yu. Beliayev, A.N. Bludov, and V.A. Horielyi

B. Verkin Institute for Low Temperature Physics and Engineering of the National Academy of Sciences of Ukraine
47 Nauky Ave., Kharkiv 61103, Ukraine
E-mail: beliayev@ilt.kharkov.ua

O.M. Osmolowskaya and M.G. Osmolowsky

Saint Petersburg State University, Institute of Chemistry
26 Universitetskii prospect, Petergof, St. Petersburg 198504, Russia

Received June 6, 2019, published online October 25, 2019

The resistive, magnetoresistive, and magnetic properties for nine compacted CrO_2 powder samples synthesized by hydrothermal method from chromic anhydride were studied. The proposed new synthesis method allows adjusting the thickness of the dielectric shells on the surface of CrO_2 nanoparticles. The powders consisted of either rounded nanoparticles (with an average diameter of ≈ 120 nm) or needle-like crystals (≈ 22.9 nm in diameter and 302 nm long). In all cases, nanoparticles were covered by dielectric shells of varied thickness and composition (for example, chromium oxide Cr_2O_3 or chromium oxyhydroxide β-CrOOH). The effect of material properties and thickness of the intergranular dielectric layers, as well as the shape of CrO_2 nanoparticles, on the magnitude of the tunnel resistance and magnetoresistance (MR) of compacted powder samples was investigated. For all the samples studied, the nonmetallic temperature behavior of the resistance and the giant negative tunneling MR were detected at low temperatures. The maximum values of MR at $T \approx 5$ K and relatively small magnetic field ($H = 0.5$ T) were approximately 37%. With increasing temperature, the MR rapidly decreased (down to ≈ 1% at $H = 1$ T, $T \approx 200$ K).

Keywords: tunnel resistance and magnetoresistance, pressed powder samples, chromium dioxide.

1. Introduction

Chromium dioxide is a ferromagnet with a Curie temperature $T_C \approx 390$ K and the calculated total magnetic moment $2\mu_B$ per formula unit [1]. This result is consistent with the experimental value obtained from the measurements of the saturated magnetization for our CrO_2 powder samples. It is almost entirely determined by the contribution of the spins and, as it is shown in [2], the calculated orbital contribution is only a few percent.

For a long time, CrO_2 has widely been used for magnetic recording. And currently, it is considered as a promising material for use in spintronics and in nanotechnology. The interest in chromium dioxide is due to the fact that it is a half-metal [3–5] having a high value of spin polarization at low enough temperatures:

$$P_e = \frac{N^{\uparrow} - N^{\downarrow}}{N^{\uparrow} + N^{\downarrow}}, \qquad (1)$$

where $N^{\uparrow}$ and $N^{\downarrow}$ are the density of states for electrons at the Fermi level with spins up ↑ and down ↓ respectively [6].

The intrinsic magnetoresistance (MR) for CrO_2 single-crystal is about 1% at room temperature in magnetic field $H = 1$ T [5]. However, for a composite granular material, which is the case for our compacted CrO_2 powder samples with nanoparticles covered by a thin dielectric layer, the MR turns out to be giant, reaching over 30% at low temperatures in low magnetic fields [4,7]. And for some of our samples, the MR value reached ~ 40% at liquid helium temperatures. The MR for such granular material is usually called extrinsic (not pertinent to the material).

Since the functionality and performance of electronic devices largely depend on the maximum of achievable tunneling MR, high MR values may be of interest for practical applications in spintronics and nanotechnology. In this regard, a comprehensive study of the influence of technological factors on the magnetoresistive properties of already known magnetic materials and, in particular, of powder systems based on CrO_2 seems to be topical.

The influence of the properties of the dielectric barrier between ferromagnets, including the properties of the ferromagnet–dielectric interfaces (and particularly the role of structural disorder in the barrier) on tunneling resistance and tunneling MR is one of the important and insufficiently studied problems of tunneling ferromagnetic junctions [5,8]. In these works, it was shown that the quality of interfaces plays an important role in tunneling. And there are some reasonable assumptions that the degree of polarization (and, consequently, the magnitude of tunneling MR) is determined not so much by the properties of a bulk ferromagnetic material, as by the properties of the surface material near the interface (or even on the verge of the ferromagnetic metal–insulator) with a thickness of several atomic layers.

Within the framework of this problem, we studied the dependence of tunnel resistance and tunnel MR in pressed CrO_2 powders on the thickness and composition of the intergranular dielectric layers, as well as on the shape of the CrO_2 nanoparticles [9–11]. The thickness, composition and properties of the dielectric layers were determined by the technology of preparation of our compacted nanopowder samples.

2. Preparation and characterization of pressed chromium dioxide nanopowders

In industry, modified chromium dioxide powders are usually synthesized by a hydrothermal method from a mixture of CrO_3, Cr_2O_3, and H_2O at the temperature ~ 350 °C and pressure ~ 40 MPa in the presence of antimony and iron catalytic compounds. In this work, the synthesis of CrO_2 was carried out by the same standard hydrothermal method. As the main stage, the chromium dioxide was synthesized from a mixture of CrO_3, water and special additives, the number and type of which determine the nucleation, growth, size and shape of particles [11,12]. We have prepared and studied several types of pressed chromium dioxide powders with needle-shaped or spherical particles. The main characteristics of the investigated powders are given in Table 1.

According to electron microscopic studies, the needle-shaped CrO_2 particles were single-crystal formations, most of them consisting of two domains, having magnetization vectors disoriented at a small angle α. The vector directed along the length of the needle-shaped particle approximately coincides with the direction of the tetragonal axis *c* that is the easy magnetization axis. When pressing tablets of particles having a needle-shaped form, these particles are mainly oriented in planes perpendicular to the applied load. For this reason, the pressed samples consisting of needle-shaped nanoparticles acquired an induced magnetic texture. At the same time, the orientation of particles in the planes can be quite arbitrary. With such particles' orientation, the projection of easy magnetization axis on the direction of the external magnetic field should be significantly larger for the longitudinal field.

The nanoparticles of which the studied powder samples were made were covered with dielectric layers of either Cr_2O_3 or β-CrOOH (chromium oxy-hydroxide) of different thickness. Both of these compounds are antiferromagnetic insulators. It is known that Cr_2O_3 has a rhombohedral lattice. It has the Neel temperature $T_N = 309$ K and exhibits a weak magnetoelectric effect.

3. The effect of the material composition and thickness of the dielectric layer on the tunnel resistance of compacted CrO_2 powders

Figure 1 shows the temperature dependences of resistivity for all samples studied. The curves numbering in this figure correspond to the sample numbers in Table 1. For all samples, we observed the temperature dependences ρ(*T*) of

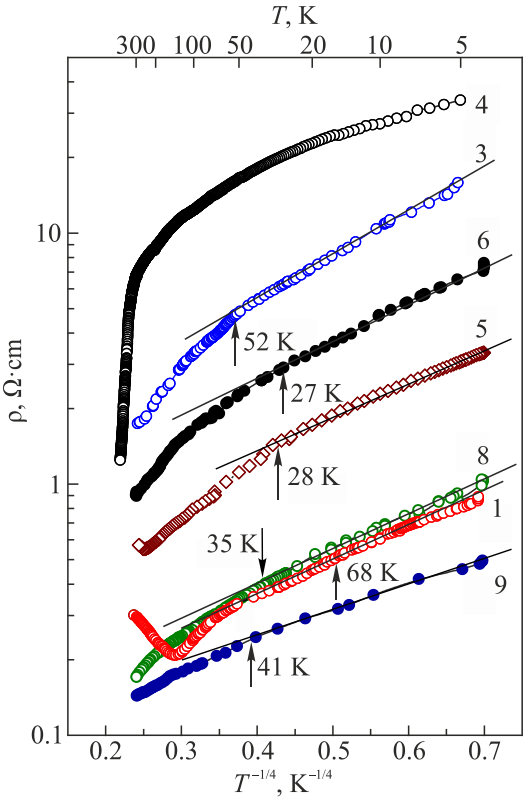

Fig. 1. Temperature dependences of the resistivity of the investigated samples of pressed CrO_2 powders. The curve numbering corresponds to the sample numbers indicated in Table 1. The arrows indicate the temperatures at which deviations from the Mott's law begin.

Table 1. The main characteristics of the studied powders

Sample number	Particle surface shell material	Shell thickness d, nm	S_{sp}, $m^2 \cdot g^{-1}$	H_c, T at $T = 293$ K	H_c, T at $T \approx 5$ K	M_{sp}, $A \cdot м^2 \cdot kg^{-1}$	M_{max}, $A \cdot м^2 \cdot kg^{-1}$ at $T = 5$ K	MR, % at $T = 5$ K
1	Naturally degraded layer (mixture of chromic acid and β-CrOOH)		~ 34	0.0429	–	78.6	–	–20 (0.6 T)
2	Cr_2O_3	1.6	~ 34	0.0421		72.5	–	–32 (0.4 T)
3	Cr_2O_3	2.1	~ 34	0.0422	0.0615	66.24	82.2	–36.6 (0.4 T)
4	Stabilized layer of β-CrOOH	3.6	10.5	0.0149	0.033	62.5	88.3	–18.6 (0.5 T)
5	β-CrOOH	1.73		0.0432	0.0609		93.6	–38.15 (0.4 T)
6	β-CrOOH	1.8		0.0429		69.7	91.2	–36 (0.15 T)
7	β -CrOOH	1.58		0.0429	0.0730	69.7	76.6 (2 T)	
8	β -CrOOH	~ 0.8		0.0522	0.0848	83.9	101.1	–36.4 (0.2 T)
9	β -CrOOH	~ 1.2		0.0761	0.1138	75.3	76.25	–26.1 (0.28 T)

Notes: S_{sp} is a specific surface area; H_c is a coercive force (at $T = 295$ K and $T \approx 5$ K), M_{sp} is a specific magnetization at room temperature in a field $H = 1$ T, M_{max} — maximum specific magnetization at low temperatures and high magnetic fields ($T \approx 5$ K, $H = 5$ T), MR — magnetoresistance, $[R(H) - R(0)]/R(0)$, at $T \approx 5$ K (in parentheses are the magnitude of the magnetic field). The MR was recorded at the measuring current $I = 100$ μA, the rate of the magnetic field alteration was $dH/dt = 0.021$ T/s. All samples consisted of needle-shaped CrO_2 nanoparticles, except the sample No. 4, consisting of rounded-shaped CrO_2 nanoparticles with an average particle diameter of ~ 120 nm. The sample No. 9 was a CrO_2 + Fe solid solution.

non-metallic type, which suggests tunneling conductivity. It can be seen that, depending on the type of dielectric layer and its thickness, the resistance of our samples may differ by two orders of magnitude.

The sample No. 4 with dense stabilized oxy-hydroxide dielectric shells (thickness $\delta = 3.6$ nm) covering the round-shaped CrO_2 nanoparticles has the highest resistance. The temperature dependence of the resistance for this sample significantly differs from one of the needle-shaped samples (for example, for $T < 20$ K it resembles the exponential one, but for $T > 20$ K it has a lower slope). So the situation with the sample No. 4 requires additional studies, but up to now we don't have other samples with round-shaped particles to compare.

For the samples with needle-shaped CrO_2 particles (Nos. 1–3 and Nos. 5–9), the dependence $\rho(T)$ at $T \leq 68$ K corresponds to the Mott's law for the 3D variable range hopping resistance: $\rho(T) \approx \rho_0 \exp(T_0 / T)^{1/4}$. At $T > 68$ K, a deviation from the Mott's law appears, and with a further increase in temperature (at $T \geq 144$ K), a transition to thermally activated conductivity occurs: the law $\rho(T) \approx \approx \rho_0 \exp(E_a/kT)$ begins to hold (see Fig. 2). Here E_a is the activation energy. The values of E_a are given in Table 2, from which it can be seen that the activation energy does not depend on the dielectric layer thickness.

Table 2. The values of activation energy E_a for CrO_2 powder samples with different shell thickness

Sample number	Shell thickness d, nm	Activation energy E_a, eV (T, K)
3	2.1	0.0102 eV (118.4 K)
6	1.8	0.0109 eV (127 K)
9	~ 1.2	0.0046 eV (53.8 K)
8	0.8	0.0122 eV (142 K)

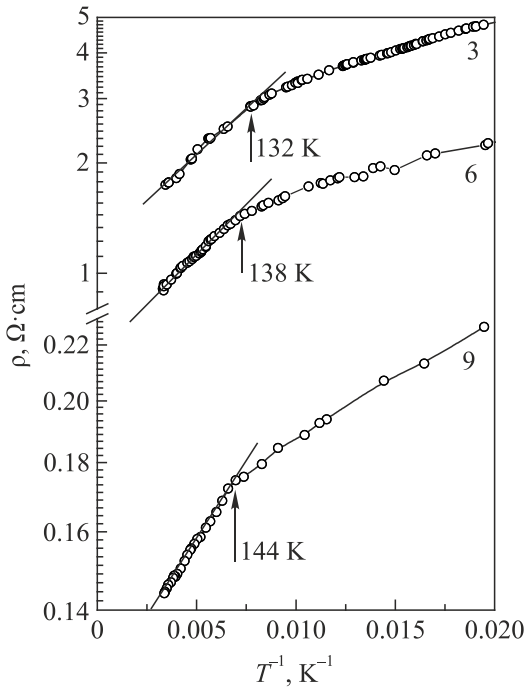

Fig. 2. Examples of ρ(*T*) dependences for three samples at high temperatures. The curve numbering corresponds to the sample numbers in Table 1.

Examining ρ(*T*) dependencies for the samples with needle-shaped particles you can see that the sample No. 3 with the thickest Cr_2O_3 dielectric interlayer (2.1 nm) has the highest resistance, and the sample No. 9 with CrO_2 particles covered with β-CrOOH dielectric oxy-hydroxide layer with the minimal thickness (~ 1.2 nm) has the lowest resistance.

At the temperature $T_{min} \approx 140$ K, the sample No. 1 exhibits a minimum of resistance and with further temperature rise a transition to metallic-type temperature dependence of resistance ($d\rho/dT > 0$) takes place. Such cases are sometimes referred to as a dielectric–metal transition with increasing temperature. Lower resistivity values for the sample No. 1 (compared to the samples Nos. 3, 5, and 6) can be associated with the thickness inhomogeneity and possible local discontinuity of the dielectric shells of particles. Such a minimum of resistance is a rather typical phenomenon in polycrystalline or granular oxides of transition metals with dielectric layers of non-uniform thickness. At low temperatures ($T < 68$ K) the ρ(*T*) values closest to those of the sample No. 1 has the sample No. 8 with the smallest thickness of the dielectric β-CrOOH covering (~ 0.8 nm). Note that both samples (No. 1 and No. 8) have the smallest thickness of the dielectric β-CrOOH covering, which accounts for the closeness of their ρ(*T*) values. The principal difference in the ρ(*T*) behavior for these two samples manifests itself only in the high-temperature region ($T > 140$ K). The resistance of the sample No. 8 with further increase in temperature continues to decrease, while for the sample No. 1, a transition to a metallic type of conductivity takes place. This transition can be associated with the degradation of the unstable dielectric shell for the sample No. 1 at sufficiently high-temperatures with further transition from activated mechanism of conductivity (in the temperature region where the Arrhenius law is fulfilled) to non-activated electron tunneling due to partial destruction of the CrO_2 particles' shells with increasing temperature that leads to formation above $T_{min} \approx 140$ K percolation channels consisting of a sequence of metal granules with weak barriers with non-activated tunneling or even simple metal "short circuits". This mechanism of resistance minimum in granular magnetic metals is described in details in [13]. Some models of such a minimum of resistance are also known (for example, [14]).

The method of Mössbauer spectroscopy on ^{57}Fe atoms has shown that Fe^{3+} ions in chromium dioxide powders (our powder No. 9) are distributed between three magnetic solid solutions [15]. In addition to $Cr_{1-x}Fe_xO_2$ solid solution (this is a massive substance and an iron-enriched surface layer) and inclusions of $Cr_{2-2x}Fe_{2x}O_3$ particles on the surface, iron is also presented in β-CrOOH chromium oxy-hydroxide, i.e., Fe atoms are also incorporated into the dielectric shell. Taking into account the results of Mössbauer spectroscopy, we believe that the lower ρ(*T*) values for the sample No. 9 than for the sample No. 8 can be associated with formation of additional localized states on iron impurities into the β-CrOOH tunneling barrier. Thus the results of ρ(*T*) measurement (Fig. 1) show that the magnitude of the tunneling resistance depends both on the type of the particles' dielectric shell and on its thickness.

The transparency coefficient *D* for a rectangular tunnel barrier with width *d* [16] is defined as

$$D \approx \exp\left\{-\frac{2\sqrt{2m}}{\hbar}\sqrt{V_0 - E}\int_{x_1}^{x_2} dx\right\} = \exp\left\{-\frac{2\sqrt{2m}}{\hbar} d\sqrt{V_0 - E}\right\}, \quad (2)$$

where $(V_0 - E)$ is the height of the barrier, and $x_2 - x_1 = d$ is the barrier thickness.

However, in the case of a more complex form of the barrier, there is no common analytical solution for calculating the coefficient *D*. Therefore, the experimental data on the effect of the type of dielectric shell of particles on the probability of electron tunneling (and tunnel resistance) are of particular interest. Both parameters (thickness of the dielectric shell and its type) are the technological parameters that can be controlled during the synthesis process thus controlling the value of the tunnel resistance. In Fig. 3 the results of measuring the temperature dependence of resistance for three samples are plotted in different coordinate systems.

Figures 3(a)–(c) demonstrate the temperature dependences ρ(*T*) for the samples with the same dielectric material (Cr_2O_3) covering the CrO_2 particles, but having the different thicknesses (2.1 and 1.6 nm).

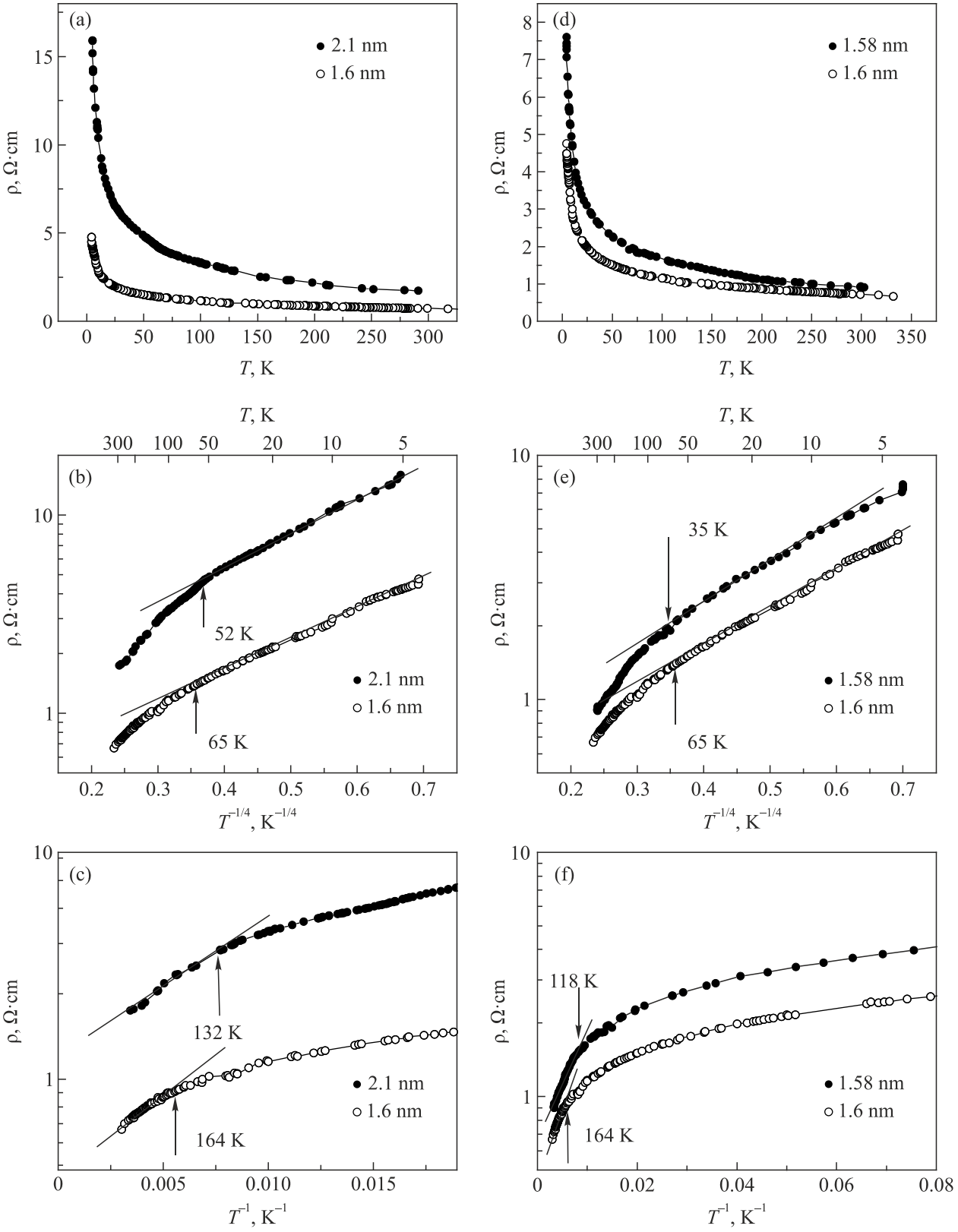

Fig. 3. (a)–(c) Temperature dependences of the resistance for two samples with the same dielectric material of different thickness, built in different coordinates: 2.1 nm Cr_2O_3 shell (sample No. 3) and 1.6 nm Cr_2O_3 shell (sample No. 2). (d)–(f) Temperature dependence of the resistance for two samples with shells made of different dielectric materials approximately the same thickness shown in different coordinates: 1.6 nm Cr_2O_3 shell (sample No. 2) and 1.58 nm β-CrOOH shell (sample No. 7).

Figures 3(d)–(f) demonstrate the temperature dependences $\rho(T)$ for the samples consisted of CrO_2 particles with different materials (Cr_2O_3 and β-CrOOH) of the dielectric shells, but having approximately the same thickness (~ 1.6 nm).

According to Fig. 3(a) the sample with a thicker dielectric layer has higher resistance. As it is known a quantum particle has a finite probability of finding it on the other side of the dielectric barrier. So the insulating layer can pass a current which is caused by a quantum tunneling through the barrier. The probability of tunneling decreases exponentially with increasing the thickness of the insulating layer (see Eq. (2)). Thus, higher resistances of the samples with thicker dielectric coatings of the particles are associated with the electrons overcoming a wider potential barrier between the FM CrO_2 granules.

In Fig. 3(b) the $\rho(T)$ dependences for the samples with different materials of dielectric coatings, but with close values of the thickness of the interlayers, also significantly differ in magnitude. In this case, the sample with higher resistance has the dielectric shell made of β-CrOOH. This can be explained either by an increase in the barrier height for this type of dielectric shells' material or by larger distortions on the interfaces in CrO_2–β-CrOOH nanoparticles' system as compared with CrO_2–Cr_2O_3 nanoparticles' system.

The presented results of $\rho(T)$ measurements show that the shell thickness has a more noticeable effect on the magnitude of the tunneling resistance (see Fig. 3) to compare with material changing. That corresponds to theoretical calculations of the transparency coefficient D according to Eq. (2). For example, the samples No. 2 and No. 3 have the same dielectric material (Cr_2O_3 shell) covering the same CrO_2 particles with different thickness. At low temperatures the values of ρ for these samples differ by about 4 times: [$\rho_{4.2\ K}$ (the sample No. 3)/$\rho_{4.2\ K}$ (the sample No. 2) ≈ 4]. The samples No. 2 and No. 7 have dielectric shells made of different materials, but with approximately the same thickness, and the ρ values for these samples in the same temperature range differ only by ~ 1.5 times [$\rho_{4.2\ K}$ (the sample No. 7)/ $\rho_{4.2\ K}$ (the sample No. 2) ≈ 1.5]. In this case, the β-CrOOH shell leads to higher resistance values (Fig. 3(b)).

More clearly, the effect of the thickness and composition of the dielectric shell on the resistance of our compacted powder samples can be seen in Fig. 4 that shows the temperature dependences of the relative difference in tunneling resistance for the samples Nos. 3 and 2 $\{(\rho_3) - (\rho_2)\}/(\rho_2)$, — (the same material, but different thickness — Fig. 4(a)), and Nos. 7 and 2 $\{(\rho_7) - (\rho_2)\}/(\rho_2)$ — (the same thickness, but different materials, Fig. 4(b)). A comparison of Fig. 4(a) and Fig. 4(b) shows that the thickness of the shell has a more pronounced effect on the value of the tunnel resistance.

This result seems trivial. At the same time, a large difference in the $\rho(T)$ values for the samples Nos. 5 and 6 (Fig. 1), that have the same β-CrOOH shell with a similar thickness, attracts attention. This result shows that the type and thickness of the dielectric shell are not the only factors determining the magnitude of the tunnel resistance. A possible reason for the different values of the tunnel resistance of these two samples with the same thickness and material of the dielectric layer is the presence of impurities and defects on CrO_2–β-CrOOH interface. The quality of interfaces is not taken into account by the theory. So, the influence of the interface properties on the ferromagnet–dielectric–ferromagnet junctions requires further study.

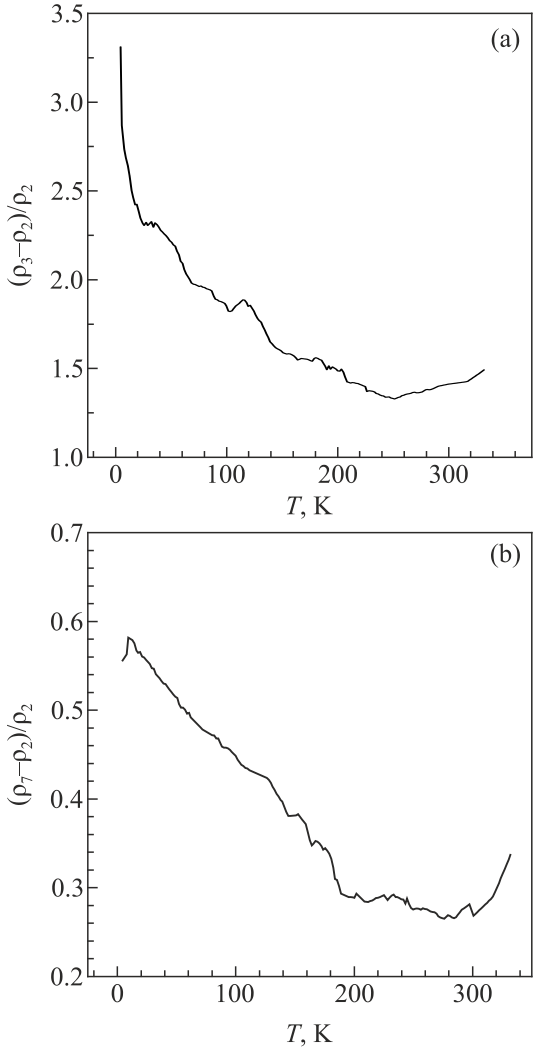

Fig. 4. (a) Temperature dependence of the relative change in the tunnel resistance with a change in the thickness of the Cr_2O_3 dielectric shell. (b) Temperature dependence of the relative change in the tunnel resistance with a change in the composition of the dielectric shell. The subscripts in the headers of the axes of the ordinates correspond to the sample numbers in the Table 1.

From our experiments, it was not possible to determine the effect of the nanoparticles' shape on the tunneling resistance value due to the lack of samples with needle-shaped particles covered by the dielectric shell with the same thickness and material as for spherical particles in sample No. 4 (~ 3.6 nm of β-CrOOH). It should be noted that the density of samples consisting of rounded CrO_2 particles is signifi-

cantly higher than that for the samples with needle-like particles (60% x-ray density vs. 40%). Based on this fact, one would expect that a higher pressing density would contribute to lowering the tunneling resistance by reducing the distance between the CrO_2 nanoparticles. However, the resistance of the sample No. 4 turned out to be significantly higher than that of the samples with needle-shaped particles (see Fig. 1).

4. Percolation effects in the conductivity of pressed powders of chromium dioxide

A part of our samples shows a transition from dielectric to metallic type of conductivity behavior with increasing temperature (Fig. 1). This transition is clearly seen for the sample No. 1. As it was mentioned above, the temperature dependence $\rho(T)$ for this sample exhibits a minimum of resistance at $T_{min} = 140$ K. A similar minimum can be observed for the sample No. 5 with $T_{min} = 250$ K. Above T_{min}, these two samples show a metallic type of temperature dependence of resistance, and below T_{min} the material behaves like a dielectric (semiconductor). At the metal-dielectric (semiconductor) transition point, the derivative $d\rho/dT$ changes its sign (see Fig. 5). In addition, it should be noted that the sample No. 3 also shows a tendency to changing the sign of derivative: at least the value of $d\rho/dT$ tends to zero with increasing temperature (Fig. 5). It is known that the studied samples consist of metal FM granules separated by dielectric layers. This implies that the transition from insulator to metallic type of conductivity behavior may be percolation by its nature. At sufficiently high temperatures, the intergranular conductivity is caused by two processes: above-barrier penetration and sub-barrier tunneling. If the activation energy (i.e. the barrier height) E_t is low enough, then at sufficiently high temperature, when $kT >> E_t$, the conductivity becomes non-activated. And in this case, the system behaves like a metal ($d\rho/dT > 0$). The lower transition temperature to the metallic type of conductivity behavior for the sample No. 1 is explained by the worse quality of it's dielectric shell — this sample has an unstabilized shell consisting of a mixture of β-CrOOH and chromic acid (see the Table 1). With increasing temperature, this shell may be partially destroyed, which leads to metallic short circuits between some of the FM granules. The second reason is the inevitable non-uniform thickness of dielectric layers, which creates prerequisites for the formation of preferable current flow channels.

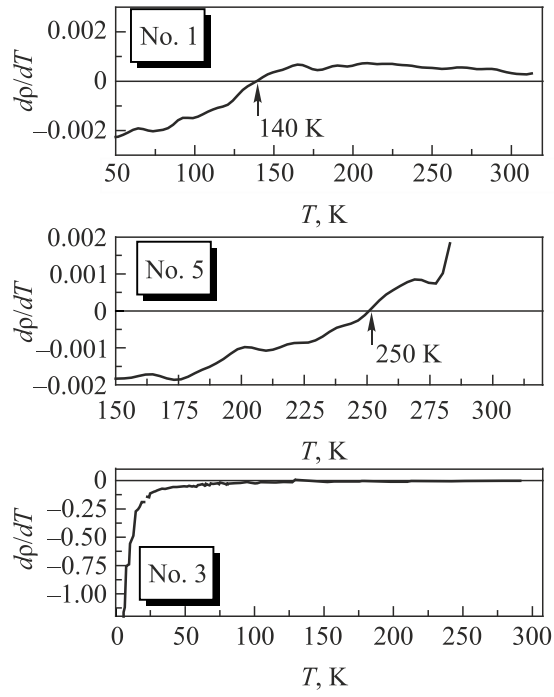

Fig. 5. The derivative of resistivity by temperature for three samples. The numbers on the graphs correspond to the numbers of the samples in Table 1.

Theoretical calculations do not contradict such ideas. For example, in [17], numerical simulations were made of low-field MR and current distribution for ferromagnetic semimetals by a random grid of resistors. The calculations performed in this work showed that there is a close relationship between the magnitude of the low-field MR and the electrical current morphology. It was shown that an increase in the degree of disorder leads to an increase in the localization of the current. In the limit of strong disorder, a quasi-one-dimensional transport channel is formed. Moreover, an increase in disorder leads to the localization of the current both in the zero field and in the final external field $H = H_{ext}$. In our case, the partial destruction of dielectric shells in the system of ferromagnetic granules when the sample is heated can be considered as an increase in the degree of disorder. Thus, our measurements show that the resistivity in the system of FM granules separated by dielectric layers may exhibit a percolation character with increasing temperature.

5. Effect of dielectric interlayer thickness on tunneling MR of pressed CrO_2 powders

Figures 6(a), (b) show the tunneling magnetoresistance (TMR) hysteresis loops for two samples with the same dielectric shells of different thickness. It can be seen that with increasing shell thickness at helium temperatures, the TMR magnitude increases very slightly. It is natural to assume that an increase in the average thickness of the intergranular layers should lead to an increase in the tunnel nature of the resistivity and to an increase in the TMR value. However, these ideas do not correspond to the results of TMR measurements for the sample No. 4 with rounded nanoparticles coated by the thickest 3.6 nm dielectric shell. The TMR magnitude for this sample is about 2 times smaller than the TMR values for the samples Nos. 3 and 5, which have thinner dielectric coatings on their particles (Figs. 6 and 7). Figures 6(c), (d) show for comparison MR curves for two samples with approximately the same thickness, but different dielectric coating material.

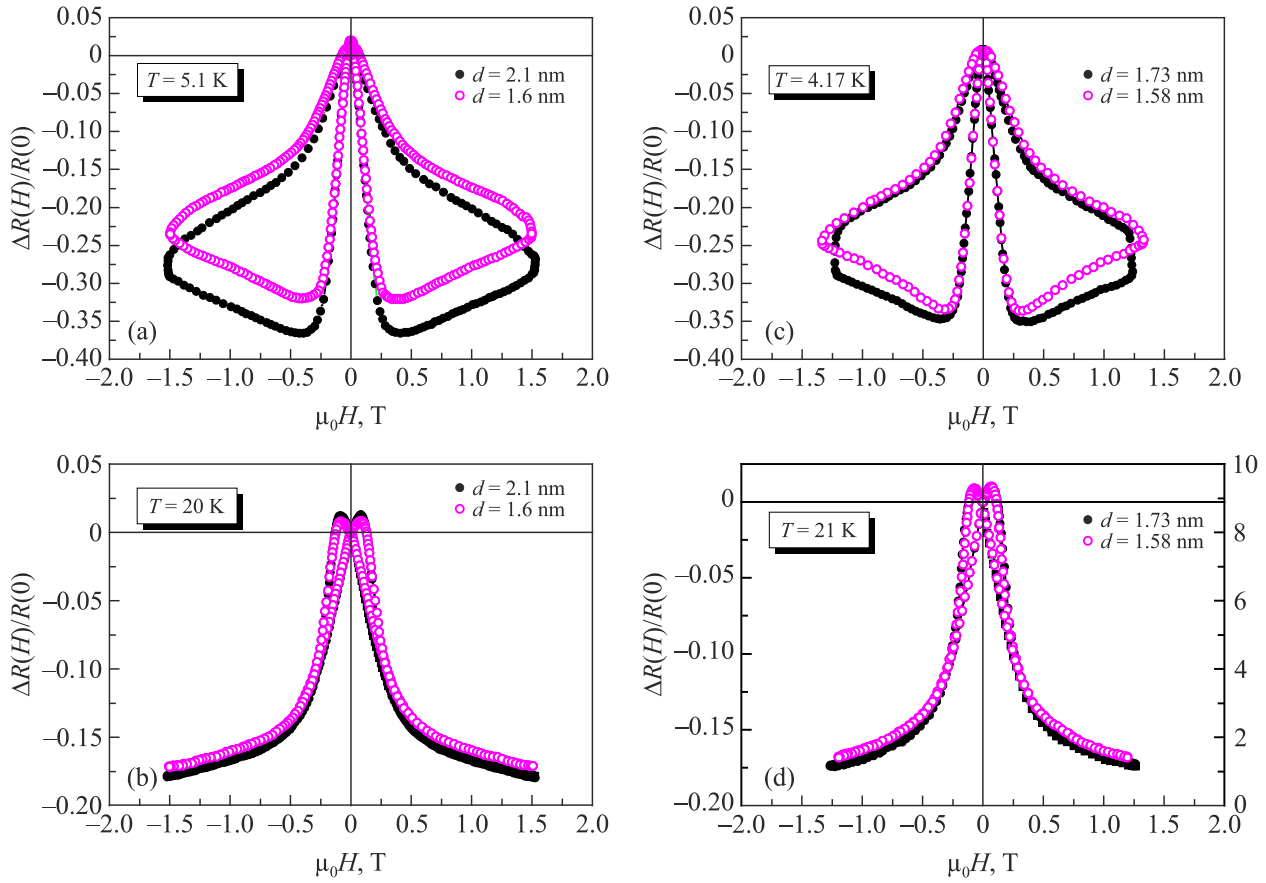

Fig. 6. Tunnel MR hysteresis loops (the magnetic field H is parallel to the sample plane): samples No. 2 and No. 3 at 5 K (a) and 20 K (b). The dielectric shell is Cr_2O_3. Samples Nos. 5 and 7 at 4.17 K (c) and 21 K (d). The dielectric shell is β-CrOOH.

In the known published data, the dependence of TMR on the thickness of the dielectric interlayers is practically not investigated, therefore, only some assumptions can be made on this account. With sufficiently thick intergranular dielectric layers, granulated samples turn into a system of completely isolated granules, in which tunneling and, accordingly, TMR should be completely absent.

Based on these considerations, it can be concluded that increase in the thickness of the intergranular layer to a critical value shall lead to a decrease in TMR. In particular, the rather low TMR value of sample No. 4 in comparison to TMR of the other samples can be explained by a rather large thickness (3.6 nm) of its intergranular layer. The second reason affecting the magnitude of the TMR of sample No. 4 is the degree of spin polarization, or the orientation of the magnetic moments of the nanoparticles.

TMR of granular ferromagnets, including the pressed CrO_2 powders, is determined only by direct tunneling of charge carriers with preservation of the spin. The processes of passing of tunnel barriers in which the spin of the charge carriers is not preserved (for example, due to the spin flips on impurities and defects or at the boundaries of the granules) do not make any contribution to the measured TMR. According to the works [3,5,18,19] the relative magnetoresistance is associated with polarization as follows:

$$\Delta R(H)/R(0) = P_e^2/(1+P_e^2), \tag{3}$$

where P_e^2 is the effective spin polarization without spin flips in the barrier during electron tunneling. By following this formula, for some of our samples (Nos. 3, 5 and 8), having at liquid helium temperature the maximum TMR value ≈ 36–38%, the calculated spin polarization achieve 75–78%. But with rising temperature, the spin polarization rapidly decrease which leads to a decreases in TMR down to 1% at $H = 1$ T, $T = 200$ K.

In [5], the following expression for tunneling MR is given:

$$\frac{\Delta\rho}{\rho} = -\frac{JP_e}{4kT}\frac{[M^2(H)-M^2(0)]}{M_s^2}, \tag{4}$$

where J is the exchange interaction constant, M_s is the saturation magnetization. It can be seen from formulas (3) and (4) that tunneling MR depends primarily on polarization. The spin polarization of electrons in each individual granule determines the direction of the magnetic moment

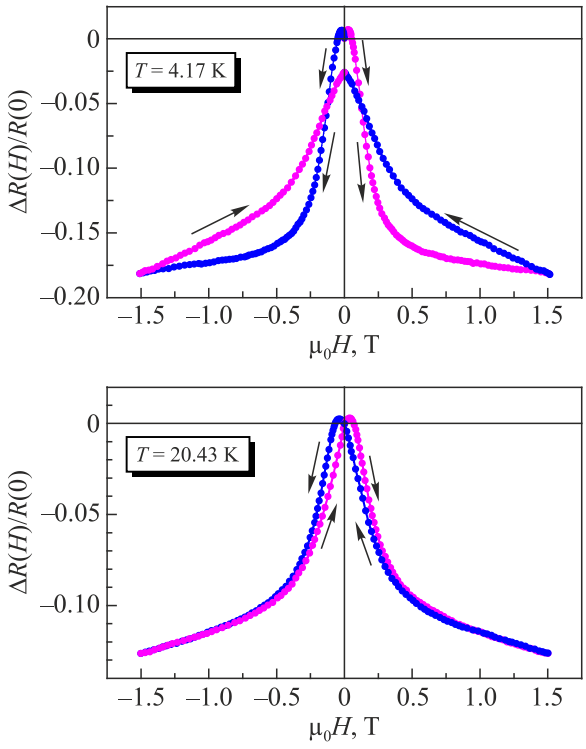

Fig. 7. Tunneling MR hysteresis loops at 4.17 K and 20.43 K for the sample No. 4 with rounded nanoparticles. Dielectric shell is β-CrOOH. The field H is parallel to the sample plane.

of this granule. In [20] it is shown that the orientation of the magnetic moments of CrO_2 nanoparticles strongly influences the TMR magnitude. In textured CrO_2 samples with needle-shaped nanoparticles, the magnetic moments of the granules are predominantly oriented in the plane of the sample. At the same time, in samples consisting of rounded nanoparticles, the direction of the magnetic moments is rather chaotic, which leads to a lower value of TMR compared to the needle-shaped powders.

From Figs. 6 and 7 it follows that an increase in temperature leads to a noticeable decrease in TMR (to ≈ 17.5% for powders with needle-shaped particles at $T \approx 20$ K). With a further increase in temperature the TMR decreases down to ~ 1% at 200 K. The main reason for this sharp decrease in TMR can be primarily explained by the disorientation of the magnetic moments of the neighboring granules and the decrease in the spin polarization P_e of CrO_2 material inside granules with increasing temperature [3–5,7,18,19,21].

In known literature, the discussion of the problem of decreasing TMR with increasing temperature is mainly qualitative. Some specific theoretical models can be found in [4,5,7,8,19,21,22]. In particular, the authors of [19] presented a phenomenological model in which it was assumed that polarization P_e is proportional to the magnetization of the surface layer of ferromagnetic particles, so that both of these quantities decrease with increasing temperature under the influence of spin-wave excitations. For the low-temperature region, the authors give the following expression [19] for $P_e(T)$:

$$P_e(T) = P_0(1 - \alpha T^{3/2}), \tag{5}$$

where P_0 is the polarization at $T = 0$ K, α is the material-dependent constant.

Another factor determining the fall of the TMR with an increase in temperature is the presence of parallel channels for the charge carriers passing through the intergranular boundaries in which the spin is not conserved. Such processes include, for example, the above-mentioned border crossing with spin-flip on impurities and lattice defects, multistage tunneling, and other processes [4,7,21]. The role of these border passage processes without preserving the spin increases with increasing temperature, which also contributes to the rapid decrease of TMR.

6. Conclusion

The resistive, magnetoresistive, and magnetic characteristics of nine compacted CrO_2 powders synthesized by the hydrothermal method were investigated. The powders consisted of rounded or needle-shaped CrO_2 nanoparticles. CrO_2 nanoparticles were coated with dielectric shells of chromium oxyhydroxide β-CrOOH or Cr_2O_3 oxide of different thicknesses. The measurement results showed that the resistance and spin-dependent tunneling MR significantly depend on the thickness and type of dielectric coating of the particles. It has been established that tunneling MR also depends on the shape of the particles.

The following features are experimentally established:

— the width of the dielectric barrier has the most noticeable effect on the magnitude of the tunnel resistance, which corresponds to theoretical concepts;

— when the Cr_2O_3 shell is replaced by the β-CrOOH shell, the probability of tunneling decreases, and the resistance increases, which may be due to more significant distortions of the interfaces in the CrO_2–β-CrOOH nanoparticles system;

— a noticeable difference in the magnitude of the tunneling resistance for two samples with the same dielectric shell of approximately equal thickness implies that the quality of the ferromagnet-dielectric interface may have a noticeable effect on the magnitude of the tunnel resistance;

— the influence of the thickness and type of the dielectric shell on the tunneling MR magnitude is insignificant. The magnitude of tunneling MR is determined primarily by the spin polarization of CrO_2 nanoparticles.

The results indicate that it is possible to control the resistive characteristics of granular systems consisting of CrO_2 nanoparticles using a controlled change in the thickness and type of dielectric interlayers. At the same time, the properties of the interfaces between the FM semimetal-dielectric-FM semimetal and their influence on the tunneling resistance and MR are not well understood and require further study.

1. K. Schwarz, *J. Phys. F* **16**, L211 (1986).
2. Yu.A. Uspenskii, E.T. Kulatov, and S.V. Halilov, *Phys. Rev. B* **54**, 474 (1996).
3. J.M.D. Coey and M. Venkatesan, *J. Appl. Phys.* **91**, 8345 (2002).
4. J.M.D. Coey, *J. Appl. Phys.* **85**, 5576 (1999).
5. M. Ziese, *Rep. Prog. Phys*. **65**, 143 (2002).
6. I.I. Mazin, *Phys. Rev. Lett*. **83**, 1427 (1999).
7. J.M.D. Coey, A.E. Berkowitz, Ll. Balcells, and F.F. Putris, *Phys. Rev. Lett*. **80**, 3815 (1998).
8. E.Y. Tsymbal, O.N. Mryasov, and P.R. LeClair, *J. Phys.: Condens. Matter* **15**, R109 (2003).
9. Yu.A. Kolesnichenko, N.V. Dalakova, E.Yu. Beliayev, O.M. Bludov, V.A. Horielyi, O.M. Osmolowskaya, and M.G. Osmolowsky, *Fiz. Nizk. Temp.* **43**, 772 (2017) [*Low Temp. Phys.* **43**, 617 (2017)].
10. N.V. Dalakova, E.Yu. Beliayev, O.M. Bludov, V.A. Gorelyi, O.M. Osmolovskaya, and M.G. Osmolovskiy, *Fiz. Nizk. Temp.* **44**, 1510 (2018) [*Low Temp. Phys.* **44**, 1180 (2018)].
11. B.I. Belevtsev, N.V. Dalakova, M.G. Osmolowsky, E.Yu. Beliayev, and A.A. Selutin, *J. Alloys Comp*. **479**, 11 (2008).
12. M.G. Osmolovsky, I.I. Kozhina, L.Yu. Ivanova, and O.L. Baydakova, *Russian J. Appl. Chem.* **74**, 1 (2001).
13. B.I. Belevtsev, D.G. Naugle, K.D.D. Rathnayaka, A. Parasiris, and J. Fink-Finowicki, *Physica B* **355**, 341 (2005).
14. A.G. Gamzatov, A.B. Batdalov, O.V. Melnikov, and O.Yu. Gorbenko, *Fiz. Nizk. Temp* **35**, 290 (2009) [*Low Temp. Phys*. **35**, 219 (2009)].
15. S.I. Bondarevskii, V.V. Eremin, V.V. Panchuk, V.G. Semenov, and M.G. Osmolovsky, *Phys. Solid State* **58**, 76 (2016).
16. L.D. Landau and L.M. Lifshitz, *Quantum Mechanics: Non-Relativistic Theory (Book 3)*, *3rd Edition*, Butterworth-Heinemann (1981).
17. Sheng Ju, Tian-Yi Cai, and Z.Y. Li, *Appl. Phys. Lett*. **87**, 172504 (2005).
18. S. Inoue and S. Maekawa, *Phys. Rev. B* **53**, R11927 (1996).
19. Chang He Shang, Janusz Nowak, Ronnie Jansen, and Jagadeesh S. Moodera, *Phys. Rev. B* **58**, R2917 (1998).
20. K. Suzuki and P.M. Tedrow, *Appl. Phys. Lett*. **74**, 428 (1999).
21. H. Liu, R.K. Zheng, Y. Wang, H.L. Bai, and X.X. Zhang, *Phys. Status Solidi A* **202**, 144 (2005).
22. H. Sun and Z.Y. Li, *Phys. Lett. A* **287**, 283 (2001).

Провідність пресованих порошків діоксиду хрому зі спін-залежним тунелюванням електронів: вплив товщини та типу діелектричних прошарків

Н.В. Далакова, Є.Ю. Біляєв, О.М. Блудов, В.О. Горєлий, О.М. Осмоловська, М.Г. Осмоловський

Досліджено резистивні, магніторезистивні та магнітні властивості для дев'яти пресованих зразків порошку CrO_2, які синтезовані гідротермальним методом з хромового ангідриду. Запропонований новий спосіб синтезу дозволяє регулювати товщину діелектричних оболонок на поверхні наночастинок CrO_2. Порошки складалися з округлих наночастинок (середній діаметр ≈ 120 нм) або голкоподібних кристалів (діаметр 22,9 нм та довжина 302 нм). У всіх випадках наночастинки покривалися діелектричними оболонками різної товщини та складу (наприклад, оксид хрому Cr_2O_3 або оксигідроксид хрому β-CrOOH). Вивчено вплив властивостей матеріалу та товщини міжгранульних діелектричних шарів, а також форми наночастинок CrO_2, на величину тунельного опору та магніторопору (МО) пресованих порошкових зразків. Для всіх досліджених зразків виявлено неметалеву температурну поведінку опору та гігантський від'ємний тунельний МО при низьких температурах. Максимальні значення МО при $T \approx 5$ К та у відносно невеликому магнітному полі ($H = 0{,}5$ Тл) становили приблизно 37%. З підвищенням температури МО швидко знижувався (до ≈ 1% при $H = 1$ Тл, $T \approx 200$ К).

Ключові слова: тунельний опір та магнітоопір, зразки пресованого порошку, діоксид хрому.

Проводимость прессованных порошков диоксида хрома со спин-зависимым туннелированием электронов: влияние толщины и типа диэлектрических прослоек

Н.В. Далакова, Е.Ю. Беляев, А.Н. Блудов, В.А. Горелый, О.М. Осмоловская, М.Г. Осмоловский

Исследованы резистивные, магниторезистивные и магнитные свойства для девяти прессованных образцов порошка CrO_2, которые синтезированы гидротермальным методом из хромового ангидрида. Предложенный новый способ синтеза позволяет регулировать толщину диэлектрических оболочек на поверхности наночастиц CrO_2. Порошки состояли из округлых наночастиц (средний диаметр ≈ 120 нм) или иглообразных кристаллов (диаметр 22,9 нм и длина 302 нм). Во всех случаях наночастицы покрывались диэлектрическими оболочками различной толщины и состава (например, оксид хрома Cr_2O_3 или оксигидроксид хрома β-CrOOH). Изучено влияние свойств материала и толщины межгранульных диэлектрических слоев, а также формы наночастиц CrO_2 на величину туннельного сопротивления и магнитосопротивления (МС) прессованных порошковых образцов. Для всех исследованных образцов обнаружены неметаллическое температурное поведение сопротивления и гигантское отрицательное туннельное МС при низких температурах. Максимальные значения МС при $T \approx 5$ К и в относительно небольшом магнитном поле ($H = 0{,}5$ Тл) составляли примерно 37%. С повышением температуры МС быстро снижалось (до ≈ 1% при $H = 1$ Тл, $T \approx 200$ К).

Ключевые слова: туннельное сопротивление и магнитосопротивление, образцы прессованного порошка, диоксид хрома.